Monthly Notices
of the
ROYAL ASTRONOMICAL SOCIETY

MNRAS **477,** 1520–1527 (2018)
Advance Access publication 2018 April 21

doi:10.1093/mnras/sty998

ExoMol line lists XXV: a hot line list for silicon sulphide, SiS

Apoorva Upadhyay, Eamon K. Conway, Jonathan Tennyson★ and Sergei N. Yurchenko
Department of Physics and Astronomy, University College London, Gower Street, London WC1E 6BT, UK

Accepted 2018 April 6. Received 2018 March 13; in original form 2018 January 16

ABSTRACT

SiS has long been observed in the circumstellar medium of the carbon-rich star IRC+10216 CW Leo. Comprehensive and accurate rotation–vibrational line lists and partition functions are computed for 12 isotopologues of silicon sulphide ($^{28}Si^{32}S$, $^{28}Si^{34}S$, $^{29}Si^{32}S$, $^{28}Si^{33}S$, $^{30}Si^{32}S$, $^{29}Si^{34}S$, $^{30}Si^{34}S$, $^{28}Si^{36}S$, $^{29}Si^{33}S$, $^{29}Si^{36}S$, $^{30}Si^{33}S$, and $^{30}Si^{36}S$) in its ground ($X\,^1\Sigma^+$) electronic state. The calculations employ an existing spectroscopically accurate potential energy curve (PEC) derived from experimental measurements and a newly computed *ab initio* dipole moment curve (DMC). The $^{28}Si^{32}S$ line list includes 10 104 states and 91 715 transitions. These line lists are available from the ExoMol website (www.exomol.com) and the CDS data base.

Key words: molecular data – opacity – astronomical data bases: miscellaneous – planets and satellites: atmospheres – stars: low-mass.

1 INTRODUCTION

Silicon sulphide is well known in space. The first detections of SiS were in the microwave region by Morris et al. (1975), emitting from the IRC+10216 molecular envelope, who deduced that SiS was in greater abundance than SiO. This was in line with Tsuji (1973) who had earlier suggested that to detect SiS in circumstellar envelopes, the abundance ratio of carbon to oxygen needs to be much greater than unity, because the abundance of SiS is a function of the [C]/[O] abundance ratio. At larger distances away from the star, SiS molecules condense on to dust grains. Silicon from the dust grains is thought to be released into gas phase via shock waves produced due to the pulsation of the star. In regions radially further still, the ultra-violet (UV) radiation in the interstellar medium dissociates the molecules, hence the abundance of SiS is expected to be low in these regions (Velilla Prieto et al. 2015).

Morris et al. (1975) concluded that the observed radio-frequency lines of molecules containing elements such as Si and S could provide information on the nuclear processes occurring in stars that are in their post- main-sequence phase. Subsequent detections of many rare isotopologues of SiS were reported by Johansson et al. (1984), Ziurys et al. (1984), Kahane et al. (1988), Cernicharo, Guelin & Kahane (2000), and Mauersberger et al. (2004). Maser emission from IRC+10216 was reported by Henkel, Matthews & Morris (1983). They observed J = 1–0 transitions of SiS in the vibrational state $v = 0$, 1, and 2 at frequencies near 18 GHz. According to Henkel et al. (1983), there is a population inversion in the J = 1–0 transition in the ground vibrational state that is responsible for the maser emission. Fonfria Exposito et al. (2006) reported the first detections of SiS maser emission from J = 15–14, J = 14–13, and J = 11–10 transitions in the ground vibrational state from IRC+10216. First reports of vibrationally excited SiS in IRC+10216 came from Turner (1987) who detected transitions within the vibrational excited $v = 1$ state. Turner (1987) concluded that the emission arises from the inner region of the circumstellar envelope that has a temperature greater than 600 K. More recently Velilla Prieto et al. (2015) observed rotational lines of SiS in high vibrational states. Using the Atacama Large Millimetre Array radio telescopes, they reported detections of rotational emission lines for excited vibrational states as high as $v = 7$; transitions for other isotopologues including $^{29}Si^{32}S$, $^{30}Si^{32}S$, $^{28}Si^{33}S$, $^{28}Si^{34}S$, $^{29}Si^{33}S$, and $^{29}Si^{34}S$ in high vibrational states were also observed. Observations of 24 rotation–vibrational lines of SiS from IRC+10216 are reported by Boyle et al. (1994) who estimated the rotational excitation temperature to be 704 ± 85 K. Considerable work continues on observing SiS spectra; for example, recently Danilovich et al. (2017) observed several lines of SiS and other S-containing species in a diverse sample of 20 AGB stars, including seven M-type stars, five S-type stars, and eight carbon stars.

The ExoMol project aims at providing line lists of spectroscopic transitions for key molecular species that are likely to be important in the atmosphere of extrasolar planets and cool stars (Tennyson & Yurchenko 2012; Tennyson et al. 2016). This is essential for the continued exploration of newly discovered astrophysical objects such as exoplanets, for which there is an increasing desire to characterize their atmospheric compositions. The methodology of the line list production for diatomics is discussed by Tennyson & Yurchenko (2017b). ExoMol has already provided rotation–vibration line lists for several silicon-containing molecules: SiO (Barton, Yurchenko & Tennyson 2013), SiH_4 (Owens et al. 2017) and SiH (Yurchenko et al. 2018b), and for several sulphur-containing molecules: CS (Paulose et al. 2015), PS (Prajapat et al. 2017), H_2S (Azzam et al. 2016), SO_2 (Underwood et al. 2016a), and SO_3 (Underwood et al. 2016b) as

★ E-mail: j.tennyson@ucl.ac.uk

well as most recently SH and SN (Yurchenko et al. 2018a). Given the astronomical importance of SiS, we present line lists for the 12 stable isotopologues of SiS applicable for temperatures up to 5000 K.

The following section discusses the available experimental and theoretical data for the SiS molecule, respectively. Section 3 describes our methodology. Section 4 presents our results and compares with previous data. Finally Section 5 briefly presents our conclusions.

2 PREVIOUS LABORATORY STUDIES

2.1 Experimental data

Barrow & Jevons (1938) first observed D $^1\Pi$ – X $^1\Sigma^+$ SiS band in the UV region from 2500 to 6500 Å. Later the E $^1\Sigma^+$– X $^1\Sigma^+$ band system was observed by Vago & Barrow (1946) in absorption at a temperature of about 1000 °C. These bands were further analysed by Barrow (1946), Barrow et al. (1961), Bredohl et al. (1975), Bredohl, Cornet & Dubois (1976), and Lakshminarayana, Shetty & Gopal (1985). Linton (1980) observed chemiluminescent following the formation of SiS molecules in the reaction of Si atoms with OCS. The spectra showed two main bands in the region 350–400 nm and 385–600 nm attributed to transitions within the $^3\Pi$ – X $^1\Sigma^+$ and $^3\Sigma^+$ – X $^1\Sigma^+$ systems, respectively.

The rotational spectrum of SiS was measured by Hoeft et al. (1969), Hoeft et al. (1970), and Tiemann et al. (1972). The permanent dipole moment in the ground state by Stark effect measurements was determined to be $\mu = 1.74 \pm 0.07$ D by Murty & Curl (1969) and also by Hoeft et al. (1969). Isotopic effects on the rotational spectrum of SiS were investigated by Tiemann et al. (1972) who obtained Born–Oppenheimer breakdown (BOB) corrections.

More recently Mueller et al. (2007) observed 300 pure rotational transitions of SiS and its 12 stable isotopic species in the vibrational ground state and vibrationally excited states. Pure rotational transitions were observed for the isotope of least abundance, $^{30}Si^{36}S$, in the ground vibrational state as well as rotational transitions in $v = 1$ for $^{28}Si^{32}S$. Frum, Engleman & Bernath (1990) recorded the rotation–vibration spectrum of SiS at 13 μm (750 cm^{-1}) using Fourier transform emission spectroscopy; they recorded seven bands for the parent isotopologue of SiS and three bands for each of the rarer isotopologues. Birk & Jones (1990) also measured the rovibrational spectrum for four isotopologues of SiS ($^{28}Si^{32}S$, $^{28}Si^{34}S$, $^{29}Si^{32}S$, $^{30}Si^{32}S$) in the ground electronic state. Further experimental data for the vibrational energy levels of the ground electronic state of SiS are provided by Nair, Singh & Rai (1965).

2.2 Theoretical data

Several *ab initio* studies have been carried out on SiS starting with Robbe, Lefebvre-Brion & Gottscho (1981) who computed spectroscopic parameters of electronic states of SiS. Potential energy curves (PECs) for the ground electronic and various excited states have been calculated by several authors. These include finite difference Hartree–Fock calculations on the ground electronic state by Muller–Plathe & Laaksonen (1989). Chattopadhyaya, Chattopadhyay & Das (2002) computed PECs for a number of lower electronic states of SiS using configuration interaction calculation with relativistic effective core potentials.

Coxon & Hajigeorgiou (1992) determined an empirical X $^1\Sigma^+$ state PEC using observed rotational– vibrational and pure rotational transition line positions. This PEC, which includes BOB corrections, is accurate within experimental error. Coxon and Hajigeorgiou's PEC and BOB corrections are used in this work. See Section 3.2 for more details.

Li et al. (1988) focused their calculations on the X $^1\Sigma^+$ electronic ground state of SiS and used multi reference configuration interaction (MRCI) level calculations to compute the dissociation energy, the equilibrium bond length, and a DMC. Li et al. (1988) obtained their best value of $\mu = 1.57$ D for the permanent dipole moment, compared to the measured value $\mu = 1.74 \pm 0.07$ D; they suggested that the addition of diffuse functions to the basis sets should account for the discrepancy between the calculated and the experimental value. Subsequently, Huzinaga, Miyoshi & Sekiya (1993) also calculated the ground electronic DMC of SiS at the self-consistent field level and obtained a value of $\mu = 2.170$ D. Maroulis et al. (2000) performed coupled cluster [CCSD(T)] and finite field many body perturbation theory calculations to obtain a permanent dipole moment value close to that of Li et al. (1988), $\mu = 1.556$ D. Shi et al. (2011) provided us (Shi & Zhu, private communication) a DMC computed at the MRCI level with a large aug-cc-pV6Z basis set that gives $\mu = 1.611$ D. Pineiro, Tipping & Chackerian (1987) provided a semi-empirical dipole moment function that they used to estimate dipole matrix elements for vibration–rotational transitions. Given the variation in theoretical dipoles and the lack of agreement with the measured values, we compute our own *ab initio* DMC, see Section 3.1.

3 METHOD

The general procedure adopted here is similar to that used by us for other closed-shell diatomics such as SiO (Barton et al. 2013), PN (Yorke et al. 2014), and CS (Paulose et al. 2015). The nuclear motion problem was solved using the program Level (Le Roy 2017). As input we have used the spectroscopically determined PEC of Coxon & Hajigeorgiou (1992), with minor adjustments caused by discretization of the PEC as described below, and an *ab initio* DMC presented below.

3.1 Dipole moment curve

Initially we tested the calculated DMC of Li et al. (2014). However, when we compared these values to those given on the Cologne Database for Molecular Spectroscopy (CDMS) data base (Müller et al. 2005; Mueller et al. 2007), we found large discrepancies in the values of the Einstein A coefficients so decided to calculate our own DMC.

Ab initio calculations of the DMC were performed using MOLPRO (Werner et al. 2012) at the CCSD(T) level with an aug-cc-pV5Z basis set for 128 points between 0.9 and 3.2 Å. The dipoles were computed using the finite field approach (see Lodi & Tennyson 2010) and stable results required using a low perturbing electric field strength of 0.00005 atomic units.

Fig. 1 compares *ab initio* DMCs. Except for the curve provided by Shi et al. (2011), all other dipole curves have been calculated as part of this study using the CCSD(T) method. Our CCSD(T) DMCs appear to drop too rapidly at large bond length. This behaviour appears to be a feature of CCSD(T) DMCs (Tennyson 2014). However, tests showed that our results are not sensitive to the DMC beyond $R = 2.8$ Å. Conversely our aug-cc-pV5Z DMC is smooth at bond lengths about an equilibrium but that due to Shi et al. (2011) is computed at fewer points and is then less smooth when the points are used directly in the nuclear motion calculation. This lack of smoothness in the DMC leads to unphysical intensities (Medvedev

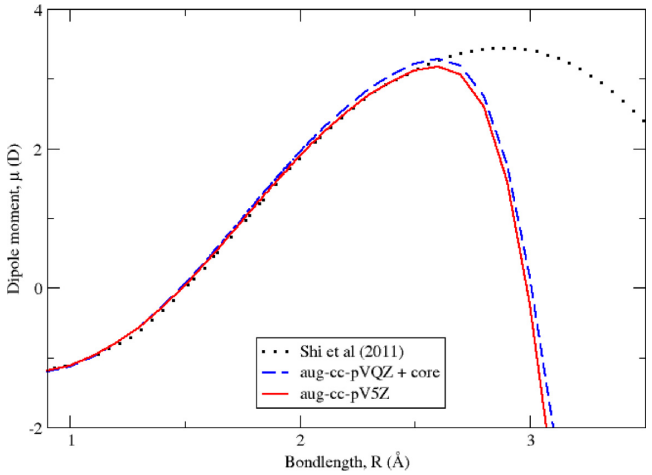

Figure 1. *Ab initio* DMCs as computed by Shi et al. (2011) and this work.

et al. 2015). Our aug-cc-pV5Z dipole points are included in the supplementary material of this article as part of the input to Level.

Einstein A coefficients were calculated using Level and our CCSD(T) aug-cc-pV5Z DMC. Our computed value of the equilibrium dipole moment is $\mu = 1.70$ D, whereas Shi et al. (2011) calculate this to be $\mu = 1.61$ D; the experimental value for the v = 0 dipole moment is $\mu = 1.74 \pm 0.07$ D. This higher value for our dipole gave better agreement with results of CDMS for pure rotational spectra, see below. Conversely all reliable DMCs considered give rather similar slopes in the region of equilibrium. This leads to a somewhat larger transition dipoles for the vibrational fundamental than the one assumed by CDMS that uses transition dipole values based on the semi-empirical estimates of Pineiro et al. (1987).

3.2 Potential energy curve

A very accurate PEC was derived by Coxon & Hajigeorgiou (1992) by fitting to spectroscopic data. The fit employed microwave and infrared data on four isotopologues (^{28}Si^{32}S, ^{28}Si^{34}S, ^{29}Si^{32}S, and ^{30}Si^{32}S) from Tiemann et al. (1972), Birk & Jones (1990), and Frum et al. (1990). The resulting PEC is valid for all isotopologues of SiS. Their Born–Oppenheimer SiS potential energy function takes the functional form of a β-variable Morse potential (Coxon & Hajigeorgiou 1991) with additional atomic mass dependent BOB terms. The effective PEC takes the form

$$U_{\rm SiS}^{\rm eff}(R) = U_{\rm SiS}^{\rm BO}(R) + \frac{1}{M_{\rm Si}} \sum_{i=1}^{3} u_i^{\rm Si}(R - R_e)^i + \frac{1}{M_{\rm S}} \sum_{i=1}^{2} u_i^{\rm S}(R - R_e)^i \quad (1)$$

where the last two terms give the functional forms of the J-independent BOB corrections for SiS. $M_{\rm Si}$ and $M_{\rm S}$ are the atomic masses of the isotopes of Si and S, respectively. Initially, Birk & Jones (1990) tried to invert their measured line positions data to a Born–Oppenheimer potential as a Dunham expansion but were unable to fit high J line positions ($J \geq 100$) that had to be excluded from the fit. Coxon & Hajigeorgiou (1992) are able to include these data in the final fit using their model.

Coxon & Hajigeorgiou (1992) showed that a small number of fitted parameters were able to represent the entire spectroscopic data set within the measurement accuracies of about 0.001 cm^{-1} for the measurements of Birk & Jones (1990) and 0.0001 cm^{-1} for the measurements of the strongest lines from Frum et al. (1990), respectively.

However, the functional form of the β-variable Morse potential is not one of those included in the Level. Therefore, the expansion parameters of the PEC given by Coxon & Hajigeorgiou (1992) were used to generate data points of the PEC that could directly input into the Level. The PEC was generated on a grid of 0.001 Å from 1.0 to 3.0 Å. These points are included in the sample Level input given in the supplementary data. As the BOB term is isotopologue dependent, it was necessary to generate a new grid of effective PEC points for each isotopologue. Tests for ^{28}Si^{32}S showed that the results, and in particular the number of vibrational states obtained, were insensitive to extending this range.

3.3 Nuclear motion calculations

Nuclear motion calculations were performed using the program Level (Le Roy 2017). All vibrational states were considered for the given PEC and isotopologue. The eigenvalues were calculated in Level using an eigenvalue convergence parameter value set to 10^{-8} cm^{-1}. Table 1 compares our results for the vibrational term values (i.e. states with $J = 0$) with the measurements of Nair et al. (1965) and the calculations of Coxon & Hajigeorgiou (1992). It can be seen that both calculations agree equally well with the observation and that there is a slight shift of about 0.003 cm^{-1} between the two theoretical calculations.

The discretization of the PEC and the minor changes in the fundamental constants used probably account for this small shift. Coxon & Hajigeorgiou (1992) remark that in order to exactly reproduce their vibrational term values the constant $h(8\pi^2 c)^{-1}$ should be set to a value of 16.8576314 amu Å^2 cm^{-1}. However in Level this constant is fixed at a value of 16.857 629 206 amu Å^2 cm^{-1}. Given that this shift is almost uniform and we are interested in the precise transition frequencies rather than energy levels, this shift was not considered important.

Table 2 compares predicted vibrational band origins for the three most important isotopically substituted SiS molecules with the results of Coxon & Hajigeorgiou (1992). Again the results show a small, almost uniform, systematic shift in the region of 0.003 cm^{-1}. Again, this difference is probably not significant.

4 LINE LISTS

4.1 Partition function

Level was used to compute all bound rotation–vibration states of each of the 12 isotopologues considered, see the summary in Table 3. Partition functions were then calculated by direct summation of all energy levels. Contributions from quasi-bound or electronically excited states were ignored. Since the nuclear spin degeneracy of both ^{28}Si and ^{32}S is zero, the nuclear spin degeneracy factor for ^{28}Si^{32}S is unity which is the value adopted by all conventions. For the other isotopologues we follow the convention adopted by HITRAN (Gamache et al. 2017) and use full integer weights given by $(2I(\mathrm{Si}) + 1)((2I(\mathrm{S}) + 1)$, where $I(X)$ is the nuclear spin of species X.

Table 4 compares our partition function for ^{28}Si^{32}S with previous compilations. The agreement is excellent. Barklem & Collet (2016) calculate their partition function values from spectroscopic constants compiled by Huber & Herzberg (1979) and Irikura (2007).

Table 1. Comparison of calculated parent isotopologue $^{28}Si^{32}S$ vibrational energy levels, in cm^{-1}, from Coxon & Hajigeorgiou (1992) (Coxon) and this work with the empirical values (Obs) of Nair et al. (1965)

v	Obs.	Coxon	This work	obs−calc	Coxon−This work
0	374.2	374.2077	374.2114	0.0	−0.0036
1	1119.0	1118.6843	1118.6877	0.3	−0.0035
2	1858.3	1857.9975	1858.0009	0.3	−0.0033
3	2592.0	2592.1534	2592.1566	−0.2	−0.0032
4	3321.8	3321.1575	3321.1606	0.6	−0.0031
5	4045.9	4045.0155	4045.0185	0.9	−0.0030
6	4763.5	4763.7328	4763.7356	−0.2	−0.0028
7	5476.9	5477.3144	5477.3171	−0.4	−0.0027
8	6181.6	6185.7655	6185.7682	−4.2	−0.0027
9	6886.8	6889.0909	6889.0936	−2.3	−0.0027
10	7587.5	7587.2953	7587.2980	0.2	−0.0027

Table 2. Comparison of vibrational energy levels, in cm^{-1}, from Coxon & Hajigeorgiou (1992) (Coxon) and this work for isotopically subsituted SiS.

	v	Coxon	This work	Coxon−This work
$^{28}Si^{34}S$	0	369.0503	369.0538	−0.0035
	1	1103.3198	1103.3231	−0.0034
	2	1832.5673	1832.5706	−0.0032
	3	2556.7986	2556.8017	−0.0031
	4	3276.0191	3276.0221	−0.0030
$^{29}Si^{32}S$	0	370.7550	370.7586	−0.0036
	1	1108.3985	1108.4019	−0.0034
	2	1840.9736	1840.9769	−0.0033
	3	2568.4860	2568.4891	−0.0031
	4	3290.9413	3290.9443	−0.0030
$^{30}Si^{32}S$	0	367.5104	367.5139	−0.0035
	1	1098.7321	1098.7354	−0.0033
	2	1824.9737	1824.9769	−0.0032
	3	2546.2409	2546.2440	−0.0031
	4	3262.5390	3262.5420	−0.0030

Table 3. Statistics for line lists for the 12 isotopologues of SiS considered in this work.

Isotopologue	v_{max}	J_{max}	Number of energies	Number of lines
$^{28}Si^{32}S$	42	257	101 04	917 15
$^{28}Si^{34}S$	42	257	102 51	942 82
$^{29}Si^{32}S$	42	257	102 04	920 03
$^{28}Si^{33}S$	42	257	101 82	919 41
$^{28}Si^{36}S$	43	257	104 23	947 51
$^{30}Si^{34}S$	43	257	104 87	949 32
$^{29}Si^{34}S$	43	257	103 87	946 58
$^{29}Si^{33}S$	42	257	102 77	943 78
$^{30}Si^{33}S$	43	257	104 11	947 09
$^{29}Si^{36}S$	43	257	105 28	950 36
$^{30}Si^{36}S$	44	257	106 63	952 94
$^{30}Si^{32}S$	43	257	103 16	945 01

In an experimental study carried out by Sanz, McCarthy & Thaddeus (2003), Dunham coefficients and BOB correction terms were determined for the SiS ground electronic state ($X\ ^1\Sigma^+$) using the Fourier transform microwave spectroscopy. These coefficients were used as spectroscopic constants by Barklem & Collet (2016) to calculate their partition function values listed in Table 4, which are in particularly good agreement with our (direct summation of energy level) values, at lower temperatures. Our partition functions for all

Table 4. Comparison of our partition function for $^{28}Si^{32}S$ with the values given in CDMS (Müller et al. 2005) and by Barklem & Collet (2016) as a function of temperature, T.

T (K)	This work	CDMS	Barklem & Collet (2016)
3.0	7.229 63	–	7.229 68
9.375	21.8566	21.8566	–
18.75	43.3764	43.3765	–
20.0	46.2461	–	46.2464
37.5	86.4222	86.4221	–
75.0	172.530	172.529	–
130.0	298.935	–	298.939
150.0	345.078	345.077	–
225.0	521.644	521.643	–
300.0	709.671	709.670	–
500.0	1303.91	1303.91	1303.94
1000.0	3519.30	3519.25	–
3000.0	237 69.6	–	237 74.3
8000.0	156 220	–	178 366

Table 5. Comparison of our predicted (Calc) transition frequencies (cm^{-1}) with experimentally obtained (Obs) values by Birk & Jones (1990) for the parent isotopologue $^{28}Si^{32}S$.

J'	J''	v'	v''	Obs	Calc	Obs−calc
88	89	1	0	679.5896	679.5905	−0.0009
6	5	1	0	748.0476	748.0478	−0.0002
99	100	2	1	665.2391	665.2403	−0.0012
116	115	2	1	787.9384	787.9391	−0.0007
6	7	3	2	729.8961	729.8963	−0.0002
69	68	3	2	768.1500	768.1498	0.0002
42	43	4	3	700.7459	700.7453	0.0006
34	33	4	3	747.5076	747.5078	−0.0001
89	90	5	4	659.1780	659.1773	0.0008
24	23	5	4	737.2133	737.2134	−0.0001
17	18	6	5	707.6352	707.6353	−0.0001
127	126	6	5	768.0828	768.0801	0.0027
20	21	7	6	700.6245	700.6236	0.0008
74	73	7	6	748.5679	748.5681	−0.0002
53	54	8	7	672.7660	672.7658	0.0002
90	89	8	7	748.4143	748.4110	0.0033
25	26	9	8	687.2477	687.2482	−0.0005
8	7	9	8	707.8742	707.8747	−0.0005
29	30	10	9	679.5703	679.5700	0.0003
19	20	10	9	686.0696	686.0688	0.0008

Table 6. Comparison of our predicted (Calc) transition frequencies (cm^{-1}) with experimentally obtained (Obs) values by Birk & Jones (1990) for isotopically subsituted SiS.

	J'	J''	v'	v''	Obs	Calc	Obs−calc
$^{28}Si^{34}S$	82	83	1	0	676.1871	676.1873	−0.0002
	24	23	1	0	747.5463	747.5470	−0.0007
	63	64	2	1	686.2286	686.2290	−0.0004
	6	5	2	1	732.7039	732.7050	−0.0010
	36	37	3	2	700.8034	700.8026	0.0008
	88	87	3	2	763.9691	763.9694	−0.0003
	49	50	4	3	686.8249	686.8243	0.0006
	26	25	4	3	733.3080	733.3081	−0.0001
$^{30}Si^{32}S$	106	107	1	0	658.7018	658.7018	0.0000
	39	38	1	0	758.5463	758.5460	0.0003
	4	5	2	1	729.5870	729.5884	−0.0014
	2	1	2	1	733.7504	733.7495	0.0009
	40	41	3	2	701.0780	701.0768	0.0012
	90	89	3	2	768.1860	768.1862	−0.0002
	54	55	4	3	686.1028	686.1023	0.0005
	26	25	4	3	736.6676	736.6676	0.0000
$^{30}Si^{32}S$	8	9	1	0	725.8659	725.8648	0.0011
	67	66	1	0	763.7698	763.7715	−0.0017
	34	35	2	1	704.2666	704.2667	−0.0001
	95	94	2	1	768.0828	768.0861	−0.0034
	21	22	3	2	707.9016	707.9028	−0.0012
	36	35	3	2	740.2007	740.1993	0.0014
	74	75	4	3	665.6780	665.6789	−0.0009
	40	39	4	3	736.9890	736.9893	−0.0003

12 isotopologues on a 1 K grid up to $T = 5000$ K are provided in the supplementary data.

For ease of use the partition functions are also fitted to the functional form proposed by Vidler & Tennyson (2000)

$$\log_{10} Q(T) = \sum_{n=0}^{8} a_n (\log_{10} T)^n. \quad (2)$$

The fitted expansion parameters for each isotopologue are given in the supplementary material. These parameters reproduce the temperature dependence of partition function of SiS with a relative root-mean-square error of 0.0076 up to $T = 5000$ K, which is the maximum temperature, for which our line list is recommended.

4.2 Transition frequencies

We initially computed all rotation–vibrational transitions in the ground electronic state, which satisfy the selection rule $\Delta J = \pm 1$, with these transitions occurring between states as high as $v = 43$ and $J = 257$. There are around 330 000 transitions in the case of $^{28}Si^{32}S$. However, given concerns with the numerical stability of the intensity of higher overtone transitions (Medvedev et al. 2015), we chose to eliminate all transitions with $\Delta v \geq 6$. This reduces each line list to less than 100 000 transitions.

Table 5 compares our computed transition frequencies with a selection of measured frequencies covering a range of vibrational and rotational states for $^{28}Si^{32}S$. The agreement is excellent; essentially within the experimental uncertainty of 0.001 cm^{-1} quoted by Birk & Jones (1990) for their measurements. Table 6 gives a similar comparison, albeit for a reduced range of vibrational states, for three isotopologues of SiS. Again agreement is within experimental error. These comparisons provide confidence about the accuracy of the lines positions in the line list.

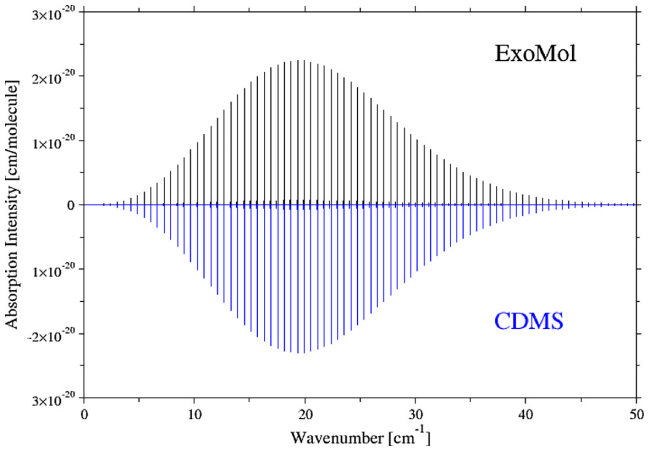

Figure 2. Comparison of our (ExoMol) pure rotational absorption spectrum of $^{28}Si^{32}S$ at $T = 300$ K in comparison with that given by CDMS.

4.3 Comparisons of spectra

In order to test the quality of our theoretical line list, we present comparisons with previous works wherever possible. For SiS the CDMS catalogue (Müller et al. 2005), rather unusually, contains both pure rotational and vibration–rotation spectra for several isotopologues of SiS. Figs 2 and 3 compare our predictions for $^{28}Si^{32}S$ with those of CDMS. For the pure rotational spectrum, Fig. 2, the agreement is excellent. CDMS is carefully designed to be highly accurate for such a long wavelength spectra and anyone wishing to study low-temperature rotational transitions of SiS is advised to start from the data in CDMS. The comparison for the vibrational fundamental, Fig. 3, is not so good. In particular our spectrum is significantly stronger than the one given by CDMS due to our *ab initio* transition dipole value (0.14 D) being slightly higher than the

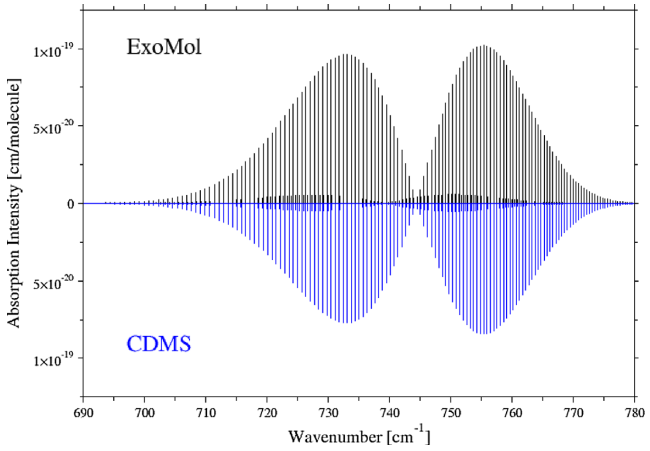

Figure 3. Comparison of our (ExoMol) absorption spectrum of $^{28}Si^{32}S$ vibrational fundamental at $T = 300$ K with that given by CDMS.

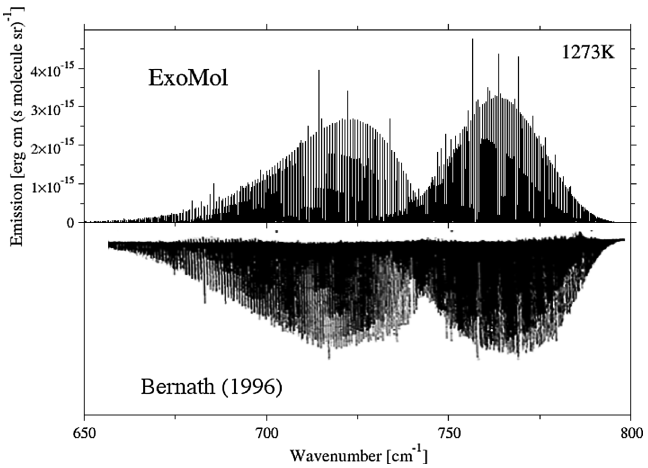

Figure 4. Comparison of our (ExoMol) emission spectrum of $^{28}Si^{32}S$ at 1000 °C with the laboratory spectrum given by Bernath (1996).

semi-empirical estimate (0.13 D) provided by Pineiro et al. (1987) for the $v = 1$–0 transition. In this case, we expect our results to be more reliable since CDMS uses a rather simple treatment of the transition dipole whereas our calculation is based on the use of a state-of-the-art dipole moment function.

There are very limited data available on hot SiS spectra. An exception is the 13 μm region; an overview emission spectrum for this region was presented by Bernath (1996) based on the measurements of Frum et al. (1990). Fig. 4 compares our predictions with this experiment. Given the relative crude nature of the observed spectrum, for which no absolute intensities are available, agreement must be regarded as satisfactory. In particular P and R branch with the vibrational band $v = 1 \rightarrow 0$, $v = 2 \rightarrow 1$, $v = 3 \rightarrow 2$, and $v = 4 \rightarrow 3$, in order of decreasing intensity, is clearly visible. Bernath (1996) notes similar features in his spectrum. We note that at higher resolution there are observable contributions from several isotopologues, as shown in Fig. 5.

4.4 Overview

In accordance with ExoMol format (Tennyson et al. 2016), the line lists are presented as two files: a states file and a transitions file. Tables 7 and 8 give brief abstracts of the $^{28}Si^{32}S$ states and transitions files, respectively. These files can be combined with the partition function, which is also provided in the data base, to give the desired spectrum at a given temperature. These files are made available for all 12 isotopologues considered at ftp://cdsarc.u-strasbg.fr/pub/cats/J/MNRAS/xxx/yy, or http://cdsarc.u-strasbg.fr/viz-bin/qcat?J/MNRAS//xxx/yy as well as the ExoMol website, www.exomol.com.

Fig. 6 presents an overview of the SiS absorption spectrum as a function of temperature.

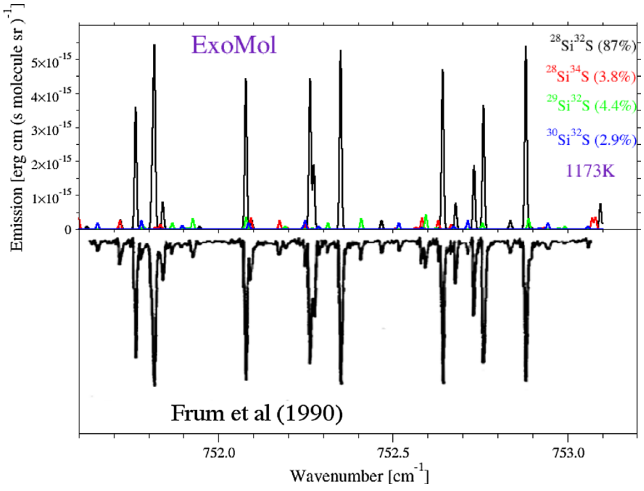

Figure 5. Comparison of our (ExoMol) emission spectrum of $^{28}Si^{32}S$ at 900 °C with the laboratory spectrum given by Frum et al. (1990). Contributions from the different isotopologues, assumed to be in natural abundance, are highlighted in our spectrum.

Table 7. Extract from the states file of the $^{28}Si^{32}S$ line list.

n	$\tilde{E}$	g_i	J	v
1	0.000 000	1	0	0
2	0.605 581	3	1	0
3	1.816 740	5	2	0
4	3.633 466	7	3	0
5	6.055 745	9	4	0
6	9.083 558	11	5	0

n: State counting number.
$\tilde{E}$: State energy in cm^{-1}.
g_i: Total statistical weight, equal to $g_{ns}(2J + 1)$.
J: Total angular momentum.
v: State vibrational quantum number.

Table 8. Extract from the transitions file of the $^{28}Si^{32}S$ line list.

f	i	A_{fi} (s^{-1})	$\tilde{\nu}_{fi}$
9972	9971	6.9703E-08	0.484 833
9854	9853	7.1086E-08	0.486 543
9713	9712	7.2306E-08	0.489 422
9552	9551	7.3278E-08	0.492 438
9374	9373	7.4098E-08	0.495 470
9179	9178	7.4809E-08	0.498 500

f: Upper state counting number.
i: Lower state counting number.
A_{fi}: Einstein-A coefficient in s^{-1}.
$\tilde{\nu}_{fi}$:Transition wavenumber in cm^{-1}.

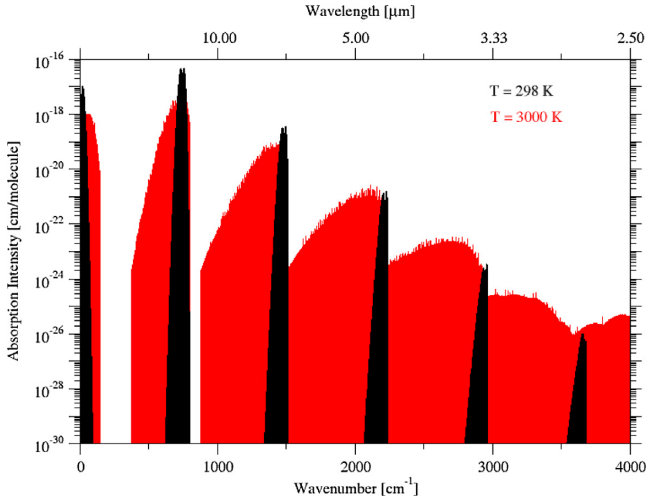

Figure 6. Temperature-dependent absorption spectrum of $^{28}Si^{32}S$.

5 CONCLUSION

Accurate and complete line lists for 12 isotopologues of SiS are presented. The line lists, which we call UCTY, use PECs based on the highly accurate study of Coxon & Hajigeorgiou (1992) and newly computed dipole moment functions. They represent the first complete line lists for these systems.

The detection of many hot rocky planets, so-called lava planets, has significantly increased the number of small molecules whose spectra may be important in exoplanet atmospheres (Tennyson & Yurchenko 2017a); SiS is one of these species. We hope that line lists such as the ones presented here will aid the characterization of exoplanetary atmospheres by planned observational missions such as ARIEL (Tinetti et al. 2018) and Twinkle (Savini et al. 2016).

ACKNOWLEDGEMENTS

This work was supported by the UK Science and Technology Research Council (STFC) grant no. ST/M001334/1 and the COST action MOLIM no. CM1405. This work made extensive use of UCL's Legion high-performance computing facility.

REFERENCES

Azzam A. A. A., Yurchenko S. N., Tennyson J., Naumenko O. V., 2016, MNRAS, 460, 4063
Barklem P. S., Collet R., 2016, A&A, 588, A96
Barrow R. F., Jevons W., 1938, Proc. Roy Soc. A, 169, 45
Barrow R. F., 1946, Proc. Phys. Soc., 58, 606
Barrow R. F., Lagerqvist A., Deutsch J. L., Westerlund B., 1961, Proc. Phys. Soc., 78, 1307
Barton E. J., Yurchenko S. N., Tennyson J., 2013, MNRAS, 434, 1469
Bernath P. F., 1996, Chem. Soc. Rev., 25, 111
Birk H., Jones H., 1990, Chem. Phys. Lett., 175, 536
Boyle R. J., Keady J. J., Jennings D. E., Hirsch K. L., Wieldemann G. R., 1994, ApJ, 420, 863
Bredohl H., Cornet R., Dubois I., Wilderia D., 1975, J. Phys. B, 8, L259
Bredohl H., Cornet R., Dubois I., 1976, J. Phys. B, 9, L207
Cernicharo J., Guelin M., Kahane C., 2000, A&AS , 142, 181
Chattopadhyaya S., Chattopadhyay A., Das K. K., 2002, J. Phys. Chem. A, 106, 833
Coxon J. A., Hajigeorgiou P. G., 1992, Chem. Phys., 167, 327
Coxon J. A., Hajigeorgiou P. G., 1991, J. Mol. Spectrosc., 150, 1
Danilovich T., Van de Sande M., De Beck E., Decin L., Olofsson H., Ramstedt S., Millar T. J., 2017, A&A, 606, A124
Fonfria Exposito J. P., Agundez M., Tercero B., Pardo J. R., Cernicharo J., 2006, ApJ, 646, L127
Frum C. I., Engleman R., Bernath P. F., 1990, J. Chem. Phys., 93, 5457
Gamache R. R. et al., 2017, J. Quant. Spectrosc. Radiat. Transf., 203, 70
Henkel C., Matthews H. E., Morris M., 1983, ApJ, 267, 184
Hoeft J., Lovas F. J., Tiemann E., Torring T., 1969, Z. Natuurforsch. A, 24, 1422
Hoeft J., Lovas F. J., Tiemann E., Torring T., 1970, J. Chem. Phys., 53, 2736
Huber K. P., Herzberg G., 1979, Molecular Spectra and Molecular Structure IV. Constants of Diatomic Molecules. Van Nostrand Reinhold Company, New York
Huzinaga S., Miyoshi E., Sekiya M., 1993, J. Comput. Chem., 14, 1440
Irikura K. K., 2007, J. Phys. Chem. Ref. Data, 36, 389
Johansson L. E. B. et al., 1984, A&A, 130, 227
Kahane C., Gomez-Gonzalez J., Cernicharo J., Guelin M., 1988, A&A, 190, 167
Lakshminarayana G., Shetty B. J., Gopal S., 1985, J. Mol. Spectrosc., 112, 1
Le Roy R. J., 2017, J. Quant. Spectrosc. Radiat. Transf., 186, 167
Li S. Z., Moncrieff D., Zhao J. G., Brown F. B., 1988, Chem. Phys. Lett., 151, 403
Li R., Zhang X.-M., Li Q.-N., Luo W., Jin M.-X., Xu H.-F., Bing Y., 2014, Acta Phys. Sin., 63, 113102
Linton C., 1980, J. Mol. Spectrosc., 80, 279
Lodi L., Tennyson J., 2010, J. Phys. B, 43, 133001
Maroulis G., Makris C., Xenides D., Karamanis P., 2000, Mol. Phys., 98, 481
Mauersberger R., Ott U., Henkel C., Cernicharo J., Gallino R., 2004, A&A, 426, 219
Medvedev E. S., Meshkov V. V., Stolyarov A. V., Gordon I. E., 2015, J. Chem. Phys., 143, 154301
Morris M., Gilmore W., Palmer P., Turner B. E., Zuckerman B., 1975, ApJ, 199, L47
Mueller H. S. P. et al., 2007, Phys. Chem. Chem. Phys., 9, 1579
Müller H. S. P., Schlöder F., Stutzki J., Winnewisser G., 2005, J. Molec. Struct. , 742, 215
Muller-Plathe F., Laaksonen L., 1989, Chem. Phys. Lett., 160, 175
Murty A. N., Curl R. F., 1969, J. Mol. Spectrosc., 30, 102
Nair K. P. R., Singh R. B., Rai D. K., 1965, J. Chem. Phys., 43, 3570
Owens A., Yurchenko S. N., Yachmenev A., Thiel W., Tennyson J., 2017, MNRAS, 471, 5025
Paulose G., Barton E. J., Yurchenko S. N., Tennyson J., 2015, MNRAS, 454, 1931
Pineiro A. L., Tipping R. H., Chackerian C., 1987, J. Mol. Spectrosc., 125, 184
Prajapat L., Jagoda P., Lodi L., Gorman M. N., Yurchenko S. N., Tennyson J., 2017, MNRAS, 472, 3648
Robbe J. M., Lefebvre-Brion H., Gottscho R. A., 1981, J. Mol. Spectrosc., 85, 215
Sanz M. E., McCarthy M. C., Thaddeus P., 2003, J. Chem. Phys., 119, 11715
Savini G. et al., 2018, Proc. SPIE, 9904, 99044M
Shi D., Xing W., Zhang X., Sun J., Zhu Z., Liu Y., 2011, Comput. Theor. Chem., 969, 17
Tennyson J., 2014, J. Mol. Spectrosc., 298, 1
Tennyson J., Yurchenko S. N., 2012, MNRAS, 425, 21
Tennyson J., Yurchenko S. N., 2017a, Mol. Astrophys., 8, 1
Tennyson J., Yurchenko S. N., 2017b, Int. J. Quantum Chem., 117, 92
Tennyson J. et al., 2016, J. Mol. Spectrosc., 327, 73
Tiemann E., Renwanz E., Hoeft J., Torring T., 1972, Z. Naturforsch. A, A27, 1566
Tinetti G. et al., 2018, Exp. Astron., in press
Tsuji T., 1973, A&A, 23, 411
Turner B. E., 1987, A&A, 183, L23
Underwood D. S., Tennyson J., Yurchenko S. N., Huang X., Schwenke D. W., Lee T. J., Clausen S., Fateev A., 2016a, MNRAS, 459, 3890

Underwood D. S., Tennyson J., Yurchenko S. N., Clausen S., Fateev A., 2016b, MNRAS, 462, 4300
Vago E. E., Barrow R. F., 1946, Proc. Phys. Soc., 58, 538
Velilla Prieto L. et al., 2015, ApJ, 805, L13
Vidler M., Tennyson J., 2000, J. Chem. Phys., 113, 9766
Werner H.-J., Knowles P. J., Knizia G., Manby F. R., Schütz M., 2012, WIREs Comput. Mol. Sci., 2, 242
Yorke L., Yurchenko S. N., Lodi L., Tennyson J., 2014, MNRAS, 445, 1383
Yurchenko S. N., Bond W., Gorman M. N., Lodi L., McKemmish L. K., Nunn W., Shah R., Tennyson J., 2018a, MNRAS , doi: 10.1093/mnras/sty939
Yurchenko S. N., Sinden F., Lodi L., Hill C., Gorman M. N., Tennyson J., 2018b, MNRAS, 473, 5324
Ziurys L. M., Cu D. P., Saykally R. J., Colvin M., Schaefer H. F., 1984, ApJ, 281, 219

SUPPORTING INFORMATION

Supplementary data are available at *MNRAS* online.

Please note: Oxford University Press is not responsible for the content or functionality of any supporting materials supplied by the authors. Any queries (other than missing material) should be directed to the corresponding author for the article.

This paper has been typeset from a TEX/LATEX file prepared by the author.